

Supporting Information: Influence of adhesion-promoting glycolipids on the structure and stability of solid-supported lipid double-bilayers

Lukas Bange,[†] Tetiana Mukhina,[†] Giovanna Fragneto,^{‡,§} Valeria Rondelli,^{*,¶}
and Emanuel Schneck^{*,†}

[†]*Institute for Condensed Matter Physics, TU Darmstadt, Hochschulstraße 8, 64289 Darmstadt,
Germany*

[‡]*Institut Laue-Langevin, Grenoble, France*

[¶]*Department of Medical Biotechnology and Translational Medicine, Università degli Studi di
Milano, Italy*

[§]*The European Spallation Source, ERIC, Lund, Sweden*

E-mail: valeria.rondelli@unimi.it; emanuel.schneck@pkm.tu-darmstadt.de

Calculation of glycolipid headgroup volumes and SLDs

Volumes of the headgroups of LacCer and Trihexo were calculated as $v_{\text{GHG}} = 419 \text{ \AA}^3$ and $v_{\text{GHG}} = 551 \text{ \AA}^3$
with the online tool *Molinspiration*,¹ based on the *smiles* representations

"C=CC(C(COC1C(C(C(C(O1)CO)OC2C(C(C(C(O2)CO)O)O)O)O)O)NC(=O)C)O"

and

"C=CC(O)C(COC3OC(CO)C(OC2OC(CO)C(OC1OC(CO)C(O)C(O)C1O)C(O)C2O)C(O)C3O)NC(C)=O"

of the headgroups of LacCer and Trihexo, respectively. The volume prediction by the molinspiration tool uses the contributions of chemical groups, which were optimized with a large training set of molecular volumes with a semi-empirical quantum-chemical method (AM1) for the calculation of molecular electronic structures. The predicted volumes are in satisfactory agreement with alternative estimates of saccharide volumes,² where each mono-saccharide has a volume of 104 cm³/mol (molinspiration: 92 cm³/mol).

The SLDs of the headgroups in H₂O and D₂O,

$$\rho_{\text{GHG}}^{\text{H}_2\text{O}}(\text{LacCer}) = 1.957 \cdot 10^{-6} \text{ \AA}^{-2}$$

$$\rho_{\text{GHG}}^{\text{D}_2\text{O}}(\text{LacCer}) = 3.747 \cdot 10^{-6} \text{ \AA}^{-2}$$

$$\rho_{\text{GHG}}^{\text{H}_2\text{O}}(\text{Trihexo}) = 2.073 \cdot 10^{-6} \text{ \AA}^{-2}$$

$$\rho_{\text{GHG}}^{\text{D}_2\text{O}}(\text{Trihexo}) = 3.935 \cdot 10^{-6} \text{ \AA}^{-2}$$

were then obtained from the total coherent scattering lengths³ per headgroup (see Eq. 2 in the main text),

$$b_{\text{tot}}^{\text{H}_2\text{O}}(\text{LacCer}) = 82.74 \text{ fm}$$

$$b_{\text{tot}}^{\text{D}_2\text{O}}(\text{LacCer}) = 157.38 \text{ fm}$$

$$b_{\text{tot}}^{\text{H}_2\text{O}}(\text{Trihexo}) = 114.24 \text{ fm}$$

$$b_{\text{tot}}^{\text{D}_2\text{O}}(\text{Trihexo}) = 216.87 \text{ fm}$$

, where all hydrogen atoms of OH groups were assumed to exchange with deuterium in the D₂O environment. With the SLDs in H₂O and D₂O at hand, the parameters *A* and *B* for Eq. 3 in the main text were calculated by solving the equations

$$\rho_{\text{GHG}}^{\text{H}_2\text{O}} = A + B\rho_{\text{H}_2\text{O}}$$

$$\rho_{\text{GHG}}^{\text{D}_2\text{O}} = A + B\rho_{\text{D}_2\text{O}}$$

, where $\rho_{\text{H}_2\text{O}} = -0.56 \cdot 10^{-6} \text{ \AA}^{-2}$ and $\rho_{\text{D}_2\text{O}} = 6.37 \cdot 10^{-6} \text{ \AA}^{-2}$, yielding

$$A = \frac{\rho_{\text{GHG}}^{\text{H}_2\text{O}}\rho_{\text{D}_2\text{O}} - \rho_{\text{GHG}}^{\text{D}_2\text{O}}\rho_{\text{H}_2\text{O}}}{\rho_{\text{D}_2\text{O}} - \rho_{\text{H}_2\text{O}}}$$

$$B = \frac{\rho_{\text{GHG}}^{\text{D2O}} - \rho_{\text{GHG}}^{\text{H2O}}}{\rho_{\text{D2O}} - \rho_{\text{H2O}}}$$

Influence of $\sigma_{\text{fluc}}^{\text{prox}}$ and $\sigma_{\text{fluc}}^{\text{dist}}$ on the volume fraction profiles

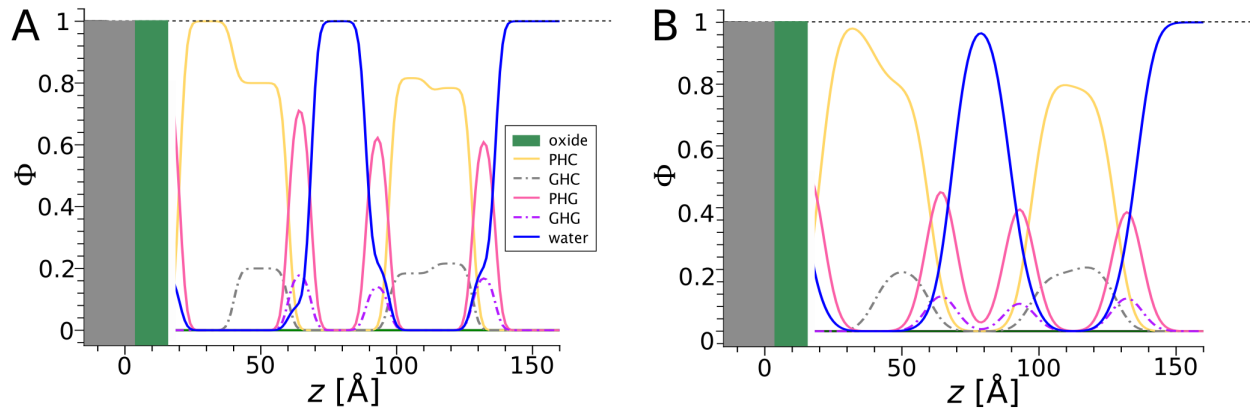


Figure S1: Volume fraction profiles for a PC/Trihexo FLB at 50°C before (A) and after (B) convolution of the bilayer-related volume fractions with Gaussian functions of widths $\sigma_{\text{fluc}}^{\text{prox}}$ and $\sigma_{\text{fluc}}^{\text{dist}}$.

Additional NR data and fits

PC FLBs

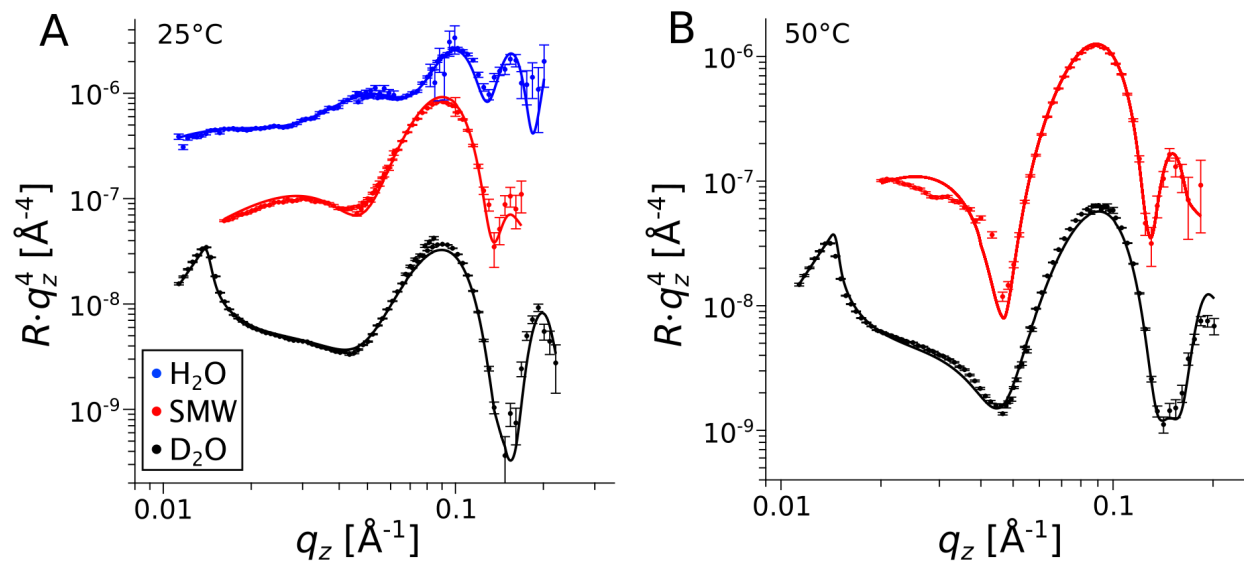


Figure S2: NR curves obtained at 25°C (A) and 50°C (B) with a PC FLB (glycolipid-free reference) based on chain-hydrogenous phospholipids. Solid lines: simulated reflectivity curves corresponding to a common volume fraction model reproducing all reflectivity curves obtained for each temperature.

PC/LacCer FLBs

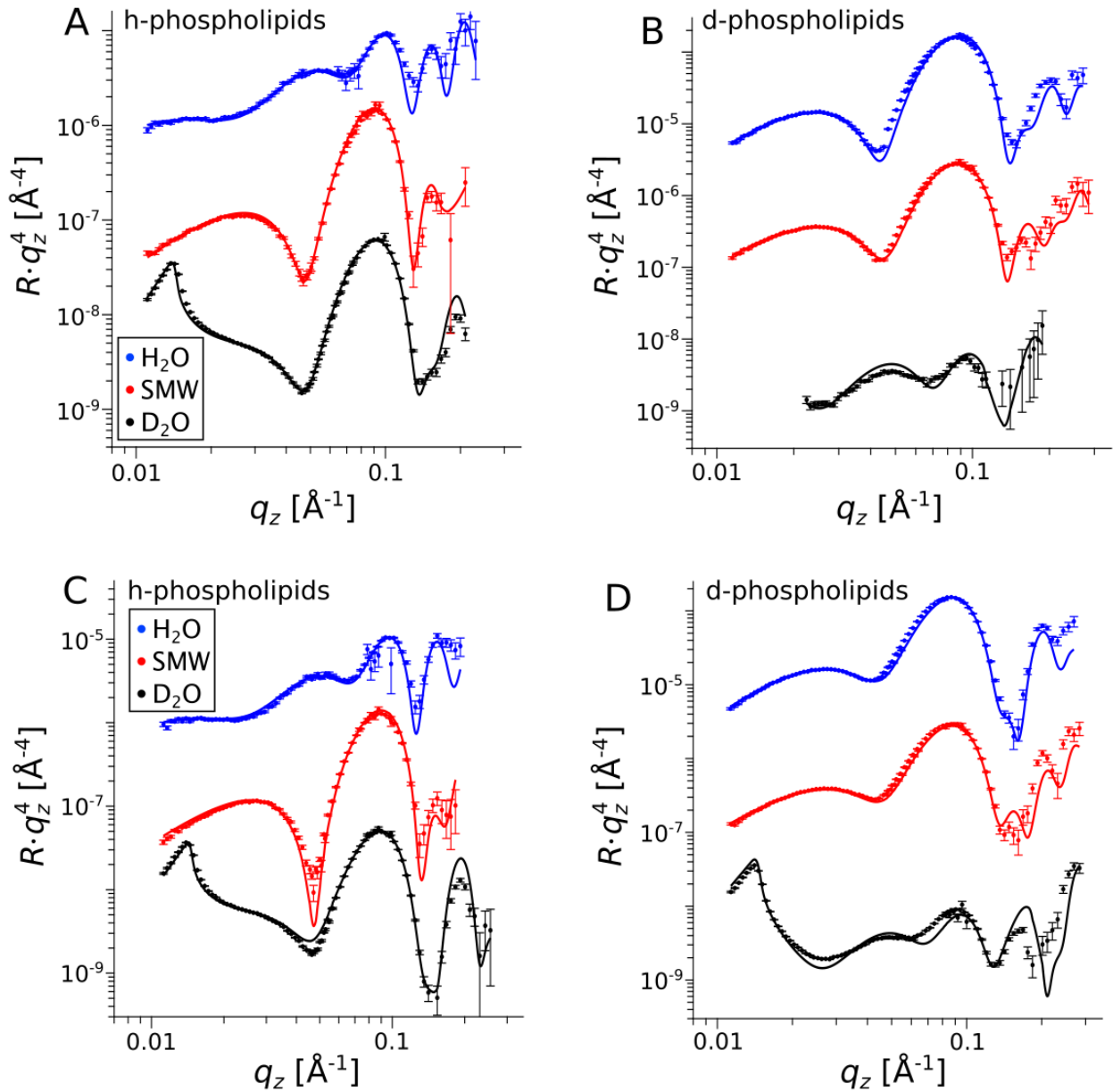


Figure S3: NR curves obtained at 50°C (A, B) and 25°C (C, D) with a PC/LacCer FLB. (A, C) Sample with chain-hydrogenous phospholipids. (B, D) Sample with chain-deuterated phospholipids. Solid lines: simulated reflectivity curves corresponding to a common volume fraction model reproducing all six reflectivity curves obtained for each temperature.

PC/Trihexo FLBs

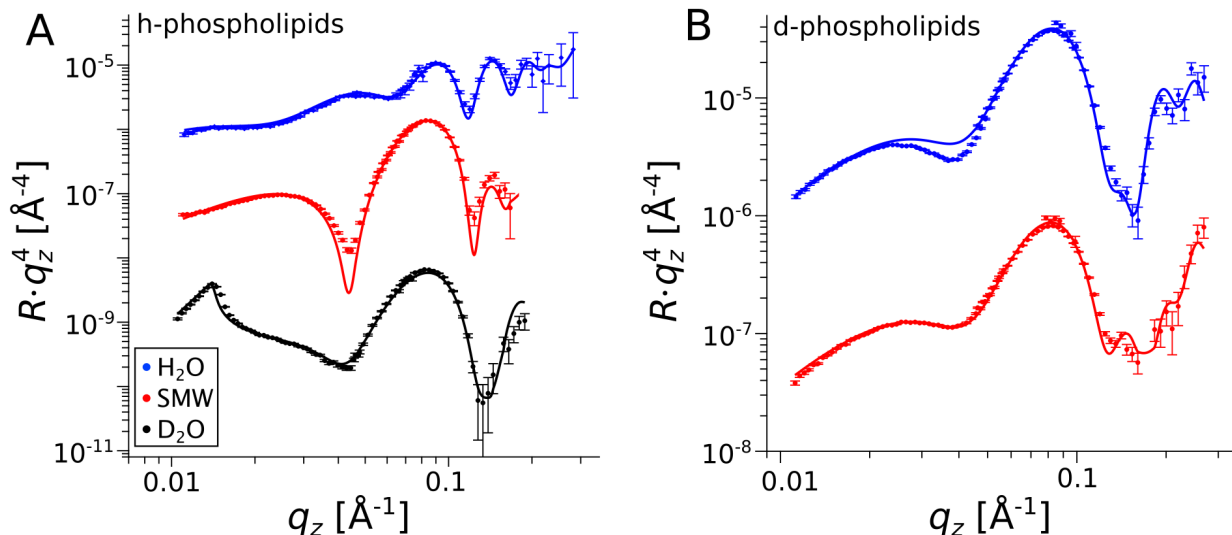


Figure S4: NR curves obtained at 25°C with a PC/Trihexo FLB. (A) Sample with chain-hydrogenous phospholipids. (B) Sample with chain-deuterated phospholipids. Solid lines: simulated reflectivity curves corresponding to a common volume fraction model reproducing all five reflectivity curves.

PC/GM1 FLBs

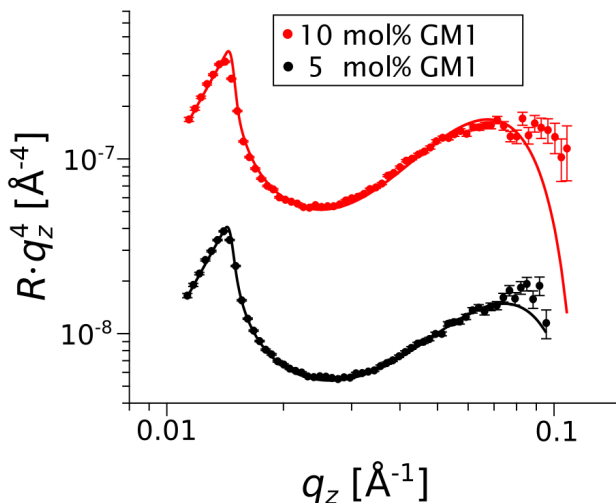


Figure S5: NR curves obtained at 25°C with PC/GM1 samples containing 10 mol% (top) or 5 mol% (bottom) GM1 in D_2O containing 100 mM NaCl. The curves are inconsistent with an FLB comprising two bilayers but consistent with a single supported lipid bilayer at both GM1 fractions. Solid lines: simulated reflectivity curves corresponding to single supported lipid bilayers.

Coherent vs. incoherent treatment of FLBs with incomplete coverage

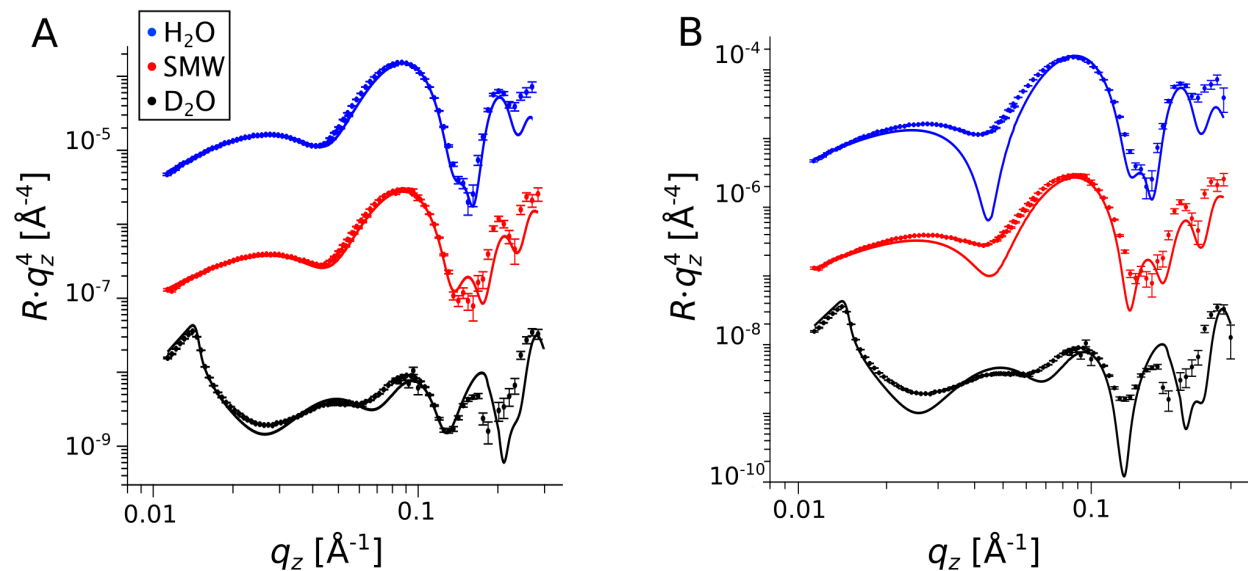


Figure S6: Comparison between incoherent (A) and coherent (B) treatments of NR data from a d-phospholipid-based PC/LacCer FLB at 25°C with incomplete coverage (see Table 3 in the main text). It is seen that the agreement is much poorer with the coherent treatment.

Hydrophobic thickness of the proximal bilayer at 25°C and 50°C

Table S1: Hydrophobic thicknesses of the proximal bilayer obtained by NR at 25°C and 50°C.

FLB sample	$2d_{\text{HC}}^{\text{prox}}, 50^\circ\text{C}$ [Å] (± 1)	$2d_{\text{HC}}^{\text{prox}}, 25^\circ\text{C}$ [Å] (± 1)
PC	38	37
PC/Trihexo	40	39
PC/LacCer	39	38
PC/GM1	40	-

Influence of an independent thickness parameter for the GHG distribution

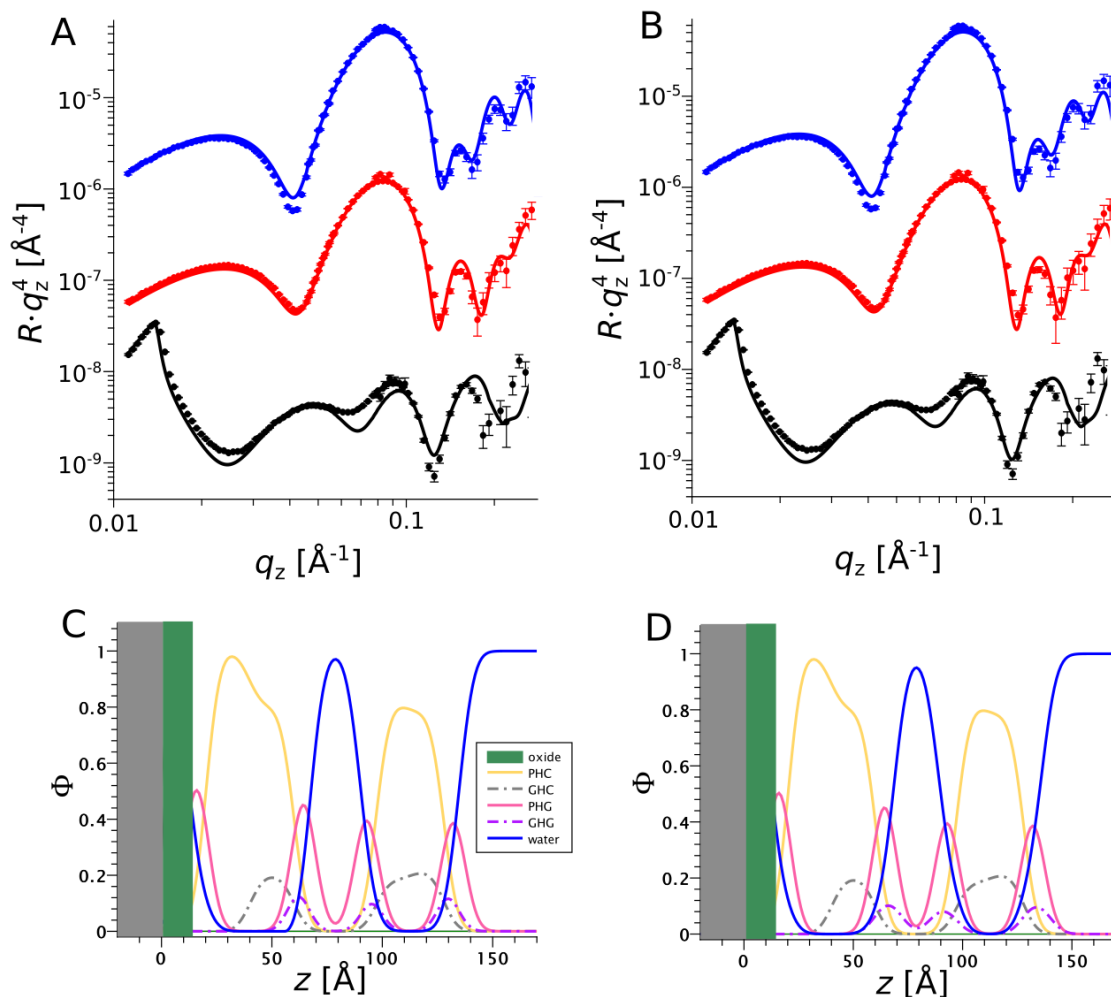


Figure S7: (A and B) NR data from a PC/Trihexo FLB with chain-deuterated PC lipids at 50°C together with the modeled reflectivity curves (solid lines) for different GHG layer thicknesses. (A) $d_{\text{GHG}} = 4 \text{ \AA}$ (B) $d_{\text{GHG}} = 12 \text{ \AA}$. These thickness values cover the entire range from a flat-on headgroup configuration to a stretched perpendicular configuration. It is seen that the modeled curves are almost insensitive to the choice of d_{GHG} . (C and D) Associated volume fraction profiles for $d_{\text{GHG}} = 4 \text{ \AA}$ (C) and $d_{\text{GHG}} = 12 \text{ \AA}$ (D).

Additional ellipsometry data

Table S2: Ellipsometric angles Δ and Ψ after transfer of three lipid layers and corresponding overall lipid layer thickness D_{lip} . Nine spots in a 3 x 3 grid pattern were chosen as measurement points to obtain an average over the block surface. System: Pure PC lipid in all three monolayers.

position on block	Δ [°]	Ψ [°]	D_{lip} [Å]
top left	150.693	11.522	92
top center	150.716	11.545	92
top right	150.974	11.598	91
mid left	151.137	11.605	90
mid center	150.547	11.479	93
mid right	150.745	11.491	92
bottom left	150.649	11.444	92
bottom center	150.416	11.444	93
bottom right	150.853	11.465	91

References

- (1) Molinspiration Cheminformatics free web services, <https://www.molinspiration.com>, Sloveny Grob, Slovakia.
- (2) Rodriguez-Loureiro, I.; Latza, V. M.; Fragneto, G.; Schneck, E. Conformation of single and interacting lipopolysaccharide surfaces bearing O-side chains. *Biophysical Journal* **2018**, *114*, 1624–1635.
- (3) Sears, V. F. Neutron scattering lengths and cross sections. *Neutron news* **1992**, *3*, 26–37.